

This is a peer-reviewed, post-print (final draft post-refereeing) version of the following published document, This is an Accepted Manuscript of an article published by Taylor & Francis in Geografiska Annaler: Series A, Physical Geography on 13 May 2020, available online: [http://www.tandfonline.com/\[Article DOI\]](http://www.tandfonline.com/[Article DOI]) and is licensed under All Rights Reserved license:

Matthews, John A, Haselberger, Stefan, Owen, Geraint, Winkler, Stefan, Hiemstra, John F, Hallang, Helen and Hill, Jennifer L ORCID logoORCID: <https://orcid.org/0000-0002-0682-783X> (2020) Snow-avalanche boulder fans in Jotunheimen, southern Norway: Schmidt-hammer exposure-age dating, geomorphometrics, dynamics and evolution. Geografiska Annaler: Series A, Physical Geography, 102 (2). pp. 118-140. doi:10.1080/04353676.2020.1762365

Official URL: <https://doi.org/10.1080/04353676.2020.1762365>
DOI: <http://dx.doi.org/10.1080/04353676.2020.1762365>
EPrint URI: <https://eprints.glos.ac.uk/id/eprint/8240>

Disclaimer

The University of Gloucestershire has obtained warranties from all depositors as to their title in the material deposited and as to their right to deposit such material.

The University of Gloucestershire makes no representation or warranties of commercial utility, title, or fitness for a particular purpose or any other warranty, express or implied in respect of any material deposited.

The University of Gloucestershire makes no representation that the use of the materials will not infringe any patent, copyright, trademark or other property or proprietary rights.

The University of Gloucestershire accepts no liability for any infringement of intellectual property rights in any material deposited but will remove such material from public view pending investigation in the event of an allegation of any such infringement.

PLEASE SCROLL DOWN FOR TEXT.

Snow-avalanche boulder fans in Jotunheimen, southern Norway: Schmidt-hammer exposure-age dating, geomorphometrics, dynamics and evolution

John A. Matthews^a, Stefan Haselberger^b, Jennifer L. Hill^c, Geraint Owen^a, Stefan Winkler^d, John F. Hiemstra^a and Helen Hallang^a

^aDepartment of Geography, College of Science, Swansea University, Singleton Park, Swansea SA2 8PP, Wales, UK

^bDepartment of Geography and Regional Research, University of Vienna, Universitätsstraße 7, 1010 Vienna, Austria

^cAcademic Development Unit, University of Gloucestershire, Cheltenham GL50 2RH, UK

^dDepartment of Geography and Geology, Julius-Maximilians-University Würzburg, Am Hubland, D-97074 Würzburg, Germany

ABSTRACT

Eleven snow-avalanche boulder fans were dated from two high-alpine sites in Jotunheimen using Schmidt-hammer exposure-age dating (SHD) and lichenometry. Average exposure ages of the surface boulders ranged from 2285 ± 725 to 7445 ± 1020 years and demonstrate the potential of SHD for dating active landforms and diachronous surfaces. Application of GIS-based morphometric analyses showed that the volume of rock material within 10 of the fans is accounted for by 16-68 % of the combined volume of their respective bedrock chutes and transport zones. It is inferred that the fans were deposited entirely within the Holocene, mainly within the early- to mid Holocene, by frequent avalanches carrying very small debris loads. Relatively small transport-zone volumes are consistent with avalanches of low erosivity. Excess chute volumes appear to represent subaerial erosion in the Younger Dryas and possibly earlier. Debris supply to the fans was likely enhanced by early-Holocene paraglacial processes following deglaciation, and by later permafrost degradation associated with the mid-Holocene Thermal Maximum. The latter, together with the

youngest SHD age from one of the fans, may presage a similar increase in geomorphic activity in response to current warming trends.

KEYWORDS

snow avalanche boulder fans

Schmidt hammer exposure age dating

high alpine permafrost degradation

paraglaciatio

periglacial geomorphology

Holocene

Introduction

Snow-avalanche boulder fans are little known depositional landforms located at the foot of steep mountain slopes in alpine periglacial environments. They were first described in detail in a classic paper by Anders Rapp (1959), who distinguished ‘avalanche boulder tongues’ from ‘talus cones’, ‘alluvial cones’ and ‘rock-slide tongues’ in northern Sweden. These snow-avalanche landforms are typically 100 to 1,000 m long, up to 200 m wide and 10 to 30 m thick with a strongly concave long profile, a basal slope angle of 10-25 ° or less, and strong size-sorting of surface debris at their distal margins where boulders with openwork texture predominate (Garner 1970; White 1981; Jomelli and Francou 2000; Owens 2004; Decaulne and Saemundsson 2006; Luckman 2013; de Haas et al. 2015). As the product of snow flow, they are clearly differentiated from debris accumulations formed by other colluvial and fluvial processes, including rock fall, debris flow and stream flow (cf. Blikra and Nemec, 1998). Typical examples under investigation in the present study are shown in Figure 1.

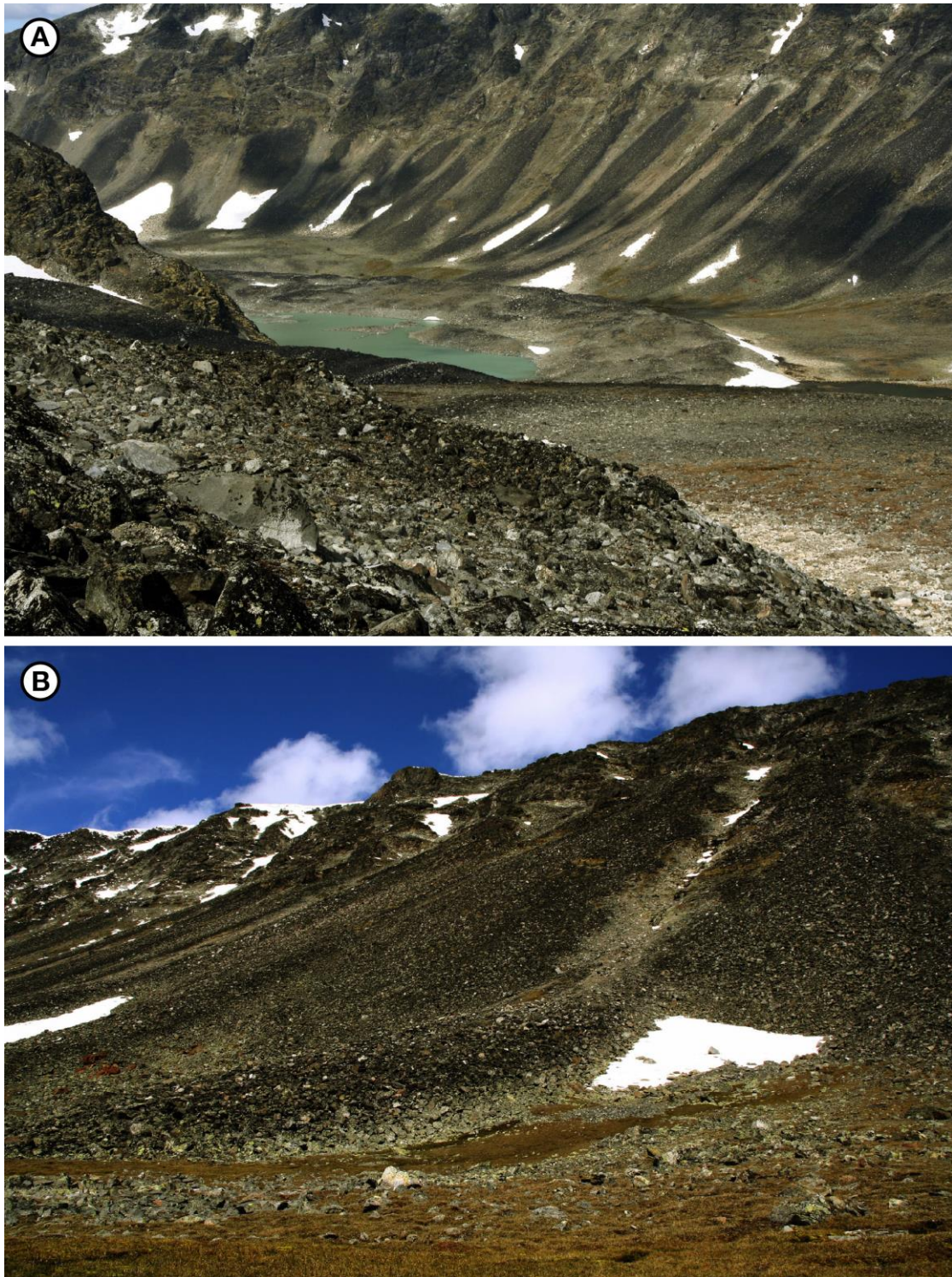


Figure 1 Snow-avalanche boulder fans in Trollsteinkvelven, Jotunheimen: (A) several fans extending onto the valley floor close to the ice-cored moraines of Grotbrean; (B) tongue-shaped fan No. 3 with a high degree of lichen cover (dark colouration) except in areas of late snow-lie (light colouration).

Rapp (1959) went on to recognise two types of avalanche boulder tongues, which he preliminarily termed ‘road-bank tongues’ and ‘fan tongues’. The former are

flat-topped, elongated and relatively steep-sided accumulations of debris extending at a low angle towards valley floors and may have asymmetrical cross-profiles. The latter extend farther from the slope foot, and are wider, thinner and less elongated features. They are consistent with being produced by relatively large snow avalanches transporting less plentiful debris along a less confined track and travelling considerably farther from the slope foot (see also Luckman 1977; Ballantyne and Harris 1994; Owens 2004; Millar 2013). In this paper we prefer not to distinguish between these two types but instead recognise transitions and variability in the form of a single class of ‘snow-avalanche boulder fans’ (cf. Luckman 1992).

Snow-avalanche boulder fans form incrementally from the accumulation of boulders and finer-grained material transported by snow avalanches down distinct bedrock chutes, gullies or couloirs (Rapp 1959; Sanders 2013). Fan surfaces display many of the small-scale landforms and sedimentary characteristics of snow-flow processes (cf. Blikra and Nemec, 1998). The fan sediments originate from the erosion of both bedrock and regolith but, as snow avalanches commonly have little erosive power and steep slopes may be almost devoid of regolith, snow avalanches tend to contain low concentrations of debris (Rapp 1960; Huber 1982; Bell et al. 1990; Jomelli and Bertran 2001; Moore et al. 2013; Ballantyne 2018), fan development is likely to be debris supply limited, and fan sediments are likely to accumulate over relatively long periods of time. The generally sparse vegetation cover and lichen size of the fan deposits may give an indication of the magnitude and frequency of recent avalanche activity affecting the fan surface (Jomelli and Pech 2004) and several generations of activity may be recognised (Decaulne 2001; Decaulne and Saemundsson 2006). However, numerical exposure-age dating of snow-avalanche boulder fans presents a significant chronological problem – especially due to their diachronous nature and the shortage of suitable organic material for radiocarbon dating in high-alpine environments.

The recent development of Schmidt hammer exposure-age dating (SHD) in southern Norway (e.g. Matthews and Owen 2010; Matthews and Winkler 2011; Matthews and McEwen 2013) provides a relatively new technique that enables the

numerical-age dating of snow-avalanche boulder fans. Although SHD has been successfully applied to many different landforms with inactive and synchronous surfaces, including moraines (Shakesby et al. 2006; Winkler 2014; Tomkins 2016, 2018), river terraces (Stahl et al. 2014), flood berms (Matthews and McEwen 2013), raised beaches (Shakesby et al. 2011) and rock-slope failures (Matthews et al. 2018; Wilson et al. 2019), there have been few applications to landforms with active and/or diachronous surfaces, such as ice-cored moraines (Matthews et al. 2014), snow-avalanche impact ramparts (Matthews et al. 2015), pronival ramparts (Matthews and Wilson 2015), patterned ground (Winkler et al. 2016, 2020) and rock glaciers (Rode and Kellerer-Pirklbauer 2011; Matthews 2013; Winkler and Lambiel 2018).

In this paper we apply SHD together with lichenometry to snow-avalanche boulder fans for the first time with the aim of improving our understanding both of these enigmatic landforms and the application of SHD in the context of active and diachronous surfaces. The three main objectives are: (1) to describe the morphology of the fans and their debris source areas using a digital elevation model (DEM); (2) to estimate the exposure age of the fan surfaces; and (3) to combine the morphological and chronological information to elucidate snow-avalanche fan dynamics and evolution.

Study area and environment

Snow-avalanche boulder fans were investigated from two high-alpine areas in central and northeastern Jotunheimen, southern Norway (Figure 2). Seven discrete fans were investigated at Trollsteinkvelven (Figure 3A) and four at Leirholet (Figure 3B). These are the best developed snow-avalanche fans known to the authors in Jotunheimen. In both areas, steep bedrock slopes with southerly aspects rise to about 2100 m above sea level, while the fan toes descend to about 1720 m a.s.l. Distinct near-parallel chutes, eroded by snow avalanches on the upper slopes, appear to coincide with steeply-dipping, macroscale, layered structures within the local geology (Battey, 1965). At Trollsteinkvelven, the fans reach the valley floor, most of which is occupied by the

ice-cored moraines of Grotbreen and the moraine-dammed lake of Trollsteintjønne (see Figure 1). At Leirholet, the fans extend onto a cirque floor that merges towards the west with a valley-side bench of Leirdalen.

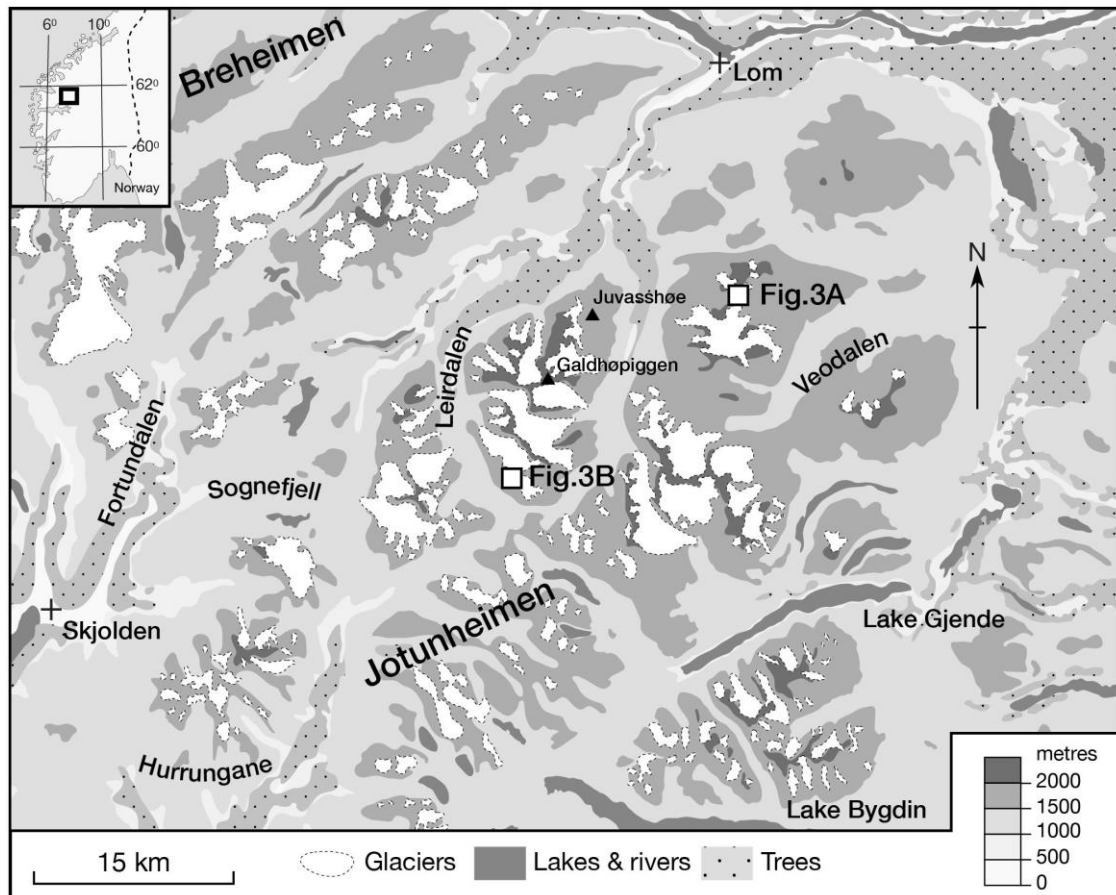


Figure 2 Location of study areas in Trollsteinkvelven (Fig. 3A) and Leirholet (Fig. 3B), Jotunheimen, southern Norway (source: <http://www.norgeskart.no>).

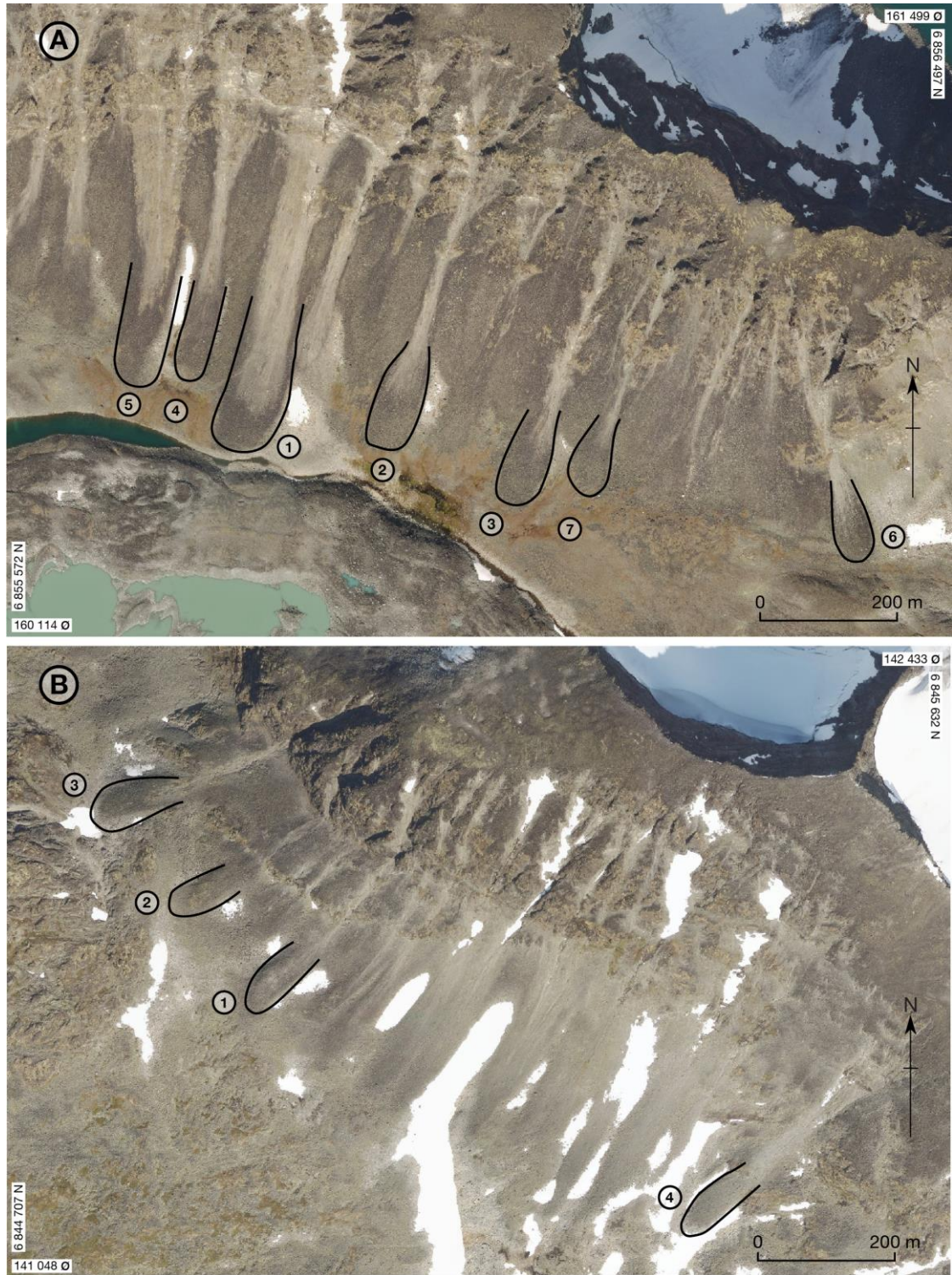


Figure 3 Aerial photographs of the study sites in (A) Trollsteinkvelven and (B) Leirholet indicating numbered snow-avalanche boulder fans. Bedrock outcrops used as 'old' control points for SHD dating are located to the SW of fan 6 in (A) and to the S of fan 3 in (B).

The metamorphic geology of the region consists primarily of pyroxene-granulite gneiss with peridotite intrusions and quartzitic veins (Battey and McRitchie 1973,

1975; Lutro and Tveten 1996). Although the gneiss is quite variable in texture, it is easily distinguished from these other lithologies. Boulders and bedrock with gneissic lithology have, moreover, successfully supported the previous development and application of SHD in the region.

All the snow-avalanche boulder fans under investigation lie within the zone of alpine permafrost, the generalized lower altitudinal limit of which lies at ~1450 m a.s.l. in the region (Ødegård et al. 1992; Isaksen et al. 2002; Farbrot et al. 2011; Lilleøren et al. 2012). In the Galdhøpiggen massif, however, the lower limit of permafrost in south-facing rockwalls is predicted to lie between 1500 and 1700 m a.s.l., which is several hundred metres higher than in rockwalls facing north (Hipp et al. 2014; Magnin et al. 2019). Thus, the depositional fans and their source areas currently lie wholly within the permafrost zone, a conclusion strengthened by available local and regional meteorological data. Mean annual air temperature for Juvasshøe (1894 m a.s.l.) for the normal period (1961-90 AD) is -4.6°C (www.met.no), with mean monthly air temperatures rising above zero only from June to September. Annual precipitation within Jotunheimen has been estimated as 800-1000 mm (Farbrot et al. 2011) with a late-summer maximum. Snowfall is relatively light in this area of Norway (www.senorge.no) and likely to result in dry- rather than wet-snow avalanches, with light debris loads and low rates of erosion (cf. Rapp 1960; Ackroyd 1986; Keylock 1997; Jomelli and Bertran 2001; Freppaz et al. 2010; Korup and Rixen 2014; Ballantyne 2018).

Small valley glaciers, cirque glaciers and ice caps are common in Jotunheimen at and around the altitude of the snow-avalanche fans (Fig. 2; Andreassen and Winsvold 2012). The history of glacier and climatic variations and their effects on the landscape are known in considerable detail. The main ice divide and ice-accumulation area of the Scandinavian Ice Sheet was located close to Jotunheimen at the maximum of the last (Weichselian) glaciation. Deglaciation of at least the main valleys is conventionally placed at ~9.7 ka, following the Late Preboreal Erdalen Event (Dahl et al. 2002). Most glaciers in Jotunheimen melted away during the Holocene Thermal Maximum (Matthews and Dresser 2008; Nesje 2009), when altitudinal permafrost

limits were also higher than today (Lilleøren et al. 2012) and there were significant effects on slope processes (e.g. Matthews et al. 2009, 2018). Neoglaciation and lowering of permafrost limits occurred during the late Holocene, culminating in the Little Ice Age of recent centuries with subsequent, continuing and accelerating glacier retreat and permafrost degradation (Matthews 2005; Matthews and Briffa 2005; Matthews and Dresser 2008; Lilleøren et al. 2012; Nesje et al. 2008).

Methodology

SHD techniques

High-resolution, calibrated SHD follows the techniques developed by Matthews and Owen (2010), Matthews and Winkler (2011) and Matthews and McEwen (2013). The approach is based on establishing a numerical, weathering-dependent relationship between Schmidt-hammer R-value and rock-surface age for a particular rock type. A linear calibration equation is derived from two control points of known age and used to produce numerical age estimates with 95% statistical confidence intervals. SHD ages predicted from the calibration equation estimate average surface exposure age and the confidence interval represents the total error (C_t), which results from combining the error associated with the calibration equation (C_c) with the sampling error associated with the dated surface (C_s). The approach and its linearity assumption are justifiable on several grounds. In particular, a linear relationship is to be expected over short timescales for resistant lithologies subject to relatively slow rates of chemical weathering in periglacial environments (André 1996; Nicholson 2008, 2009; Matthews and Owen 2011; Matthews et al. 2016), and this has been tested empirically over the Holocene timescale (Shakesby et al. 2011; Tomkins et al. 2018).

Calibration equations were established separately for Trollsteinkvelven and Leirholet. Each calibration equation was constructed from an ‘old’ and a ‘young’ control point, both involving pyroxene-granulite lithologies only. The ‘old’ control

points were glacially-scoured bedrock outcrops located within 200 m and 100 m of snow-avalanche boulder fans in Trollsteinkvelven and Leirholet, respectively. ‘Old’ control points were assigned an exposure age of ~9.7 ka, which is the conventional age of deglaciation in central Jotunheimen according to basal radiocarbon dates from mires and lakes (Karlén and Matthews 1992; Barnett et al. 2000; Nesje and Dahl 2001; Matthews et al. 2005; Hormes et al. 2009; summarized in Matthews et al. 2018) and is consistent with large-scale modeling of deglaciation in southern Norway (e.g. Hughes et al. 2016; Stroeven et al. 2016).

The ‘young’ control points were fresh, unweathered boulders scattered over fan surfaces, which were assigned an exposure age of 20 years based on the absence of yellow-green crustose lichens of the *Rhizocarpon* subgenus. Lichenometric studies within Jotunheimen indicate that about 20 years is necessary for colonization of newly exposed rock surfaces by this group of lichens (Matthews 2005; Matthews and Vater 2015). Use of these ‘young’ control points is considered highly appropriate in the context of dating snow-avalanche boulder fans because rough, unweathered surfaces of boulders of colluvial origin yield much lower R-values than smooth bedrock or boulder surfaces produced by fluvial or glacial erosion (Matthews and McEwen 2013; Matthews et al. 2018; Olsen et al. 2019).

Schmidt-hammer R-values were measured with N-type mechanical Schmidt hammers (Proceq 2004; Winkler and Matthews 2014). For ‘old’ control points, sample size (n) was 300 impacts, taken from several different areas of the bedrock outcrops. For ‘young’ control points, n was 100 boulders (two impacts per boulder). Relatively high variability of R-values from the ‘old’ control points necessitated the larger sample size, while the sample size for ‘young’ control points was limited by the scarcity of unweathered boulders on the fans. Unweathered boulders for the ‘young’ control points were sampled from four fans in Trollsteinkvelven and three of those in Leirholet. For dating each fan surface, sampling was concentrated around the distal margins where boulders were most abundant and also likely to be oldest in terms of their surface exposure age. Again, n was 100 boulders with two impacts per boulder.

Precautions were taken to minimize possible uncertainties and measurement errors, including avoiding small and/or unstable boulders, steeply sloping boulder surfaces, edges of boulders and outcrops, joints and cracks, unusual lithologies (peridotite and quartzite in this study), and wet and lichen-covered rock surfaces (cf. Shakesby et al. 2006; Matthews and Owen 2010; Viles et al. 2011). The two Schmidt hammers used had been recently recalibrated by the manufacturer and were regularly checked for deterioration throughout the study on the manufacturer's test anvil. Rock surfaces were not cleaned or artificially abraded as this would have reduced age-related weathering effects (cf. Viles et al. 2011; Moses et al. 2014).

Lichenometry

Lichenometry was used as a relative-age dating technique in support of SHD. The long axes of the ten largest thalli of the *Rhizocarpon* subgenus were measured from the distal zone of each fan, where the largest and hence oldest boulder exposure ages can be expected (cf. Jomelli and Pech 2004). The size of the single largest, five largest and ten largest lichens were assessed in relation to established indirect lichenometric dating curves from central and eastern Jotunheimen (Matthews 2005) and directly measured lichen growth rates from southern Norway (Trenbith and Matthews 2010; Matthews and Trenbith 2011).

DEM analyses

A DEM was used to establish the morphology of the fans and associated landforms. The main focus was on estimating the volume of the fans and the corresponding volume of rock material eroded upslope of the fans. GIS analyses were carried out on two publicly available DEMs from the Norwegian mapping authority, Kartverket (hoydedata.no), based on a 2013 airborne laser-scanning survey at 1 m resolution for the northern Gudbrandsdalen area. All analyses were carried out with either ArcGIS Pro 2.1 (ESRI 2017) or QGIS 3.10 (QGIS Development Team 2019).

Using field observation supported by visual comparison with the orthoimage and hillshading, as well as cross-profiles, three zones were delineated for each feature (Figure 4). The snow-avalanche source area comprises the chute and transfer zones, while the depositional area is defined as the fan zone. Polygon maps were generated and used subsequently for geomorphometric analyses. Three profile graphs were generated for each feature: a *long profile* for the whole landform assemblage, from the top of the chute to the toe of the fan; and two *cross profiles*, one across the proximal fan and the other across the distal fan, where it was at its widest.

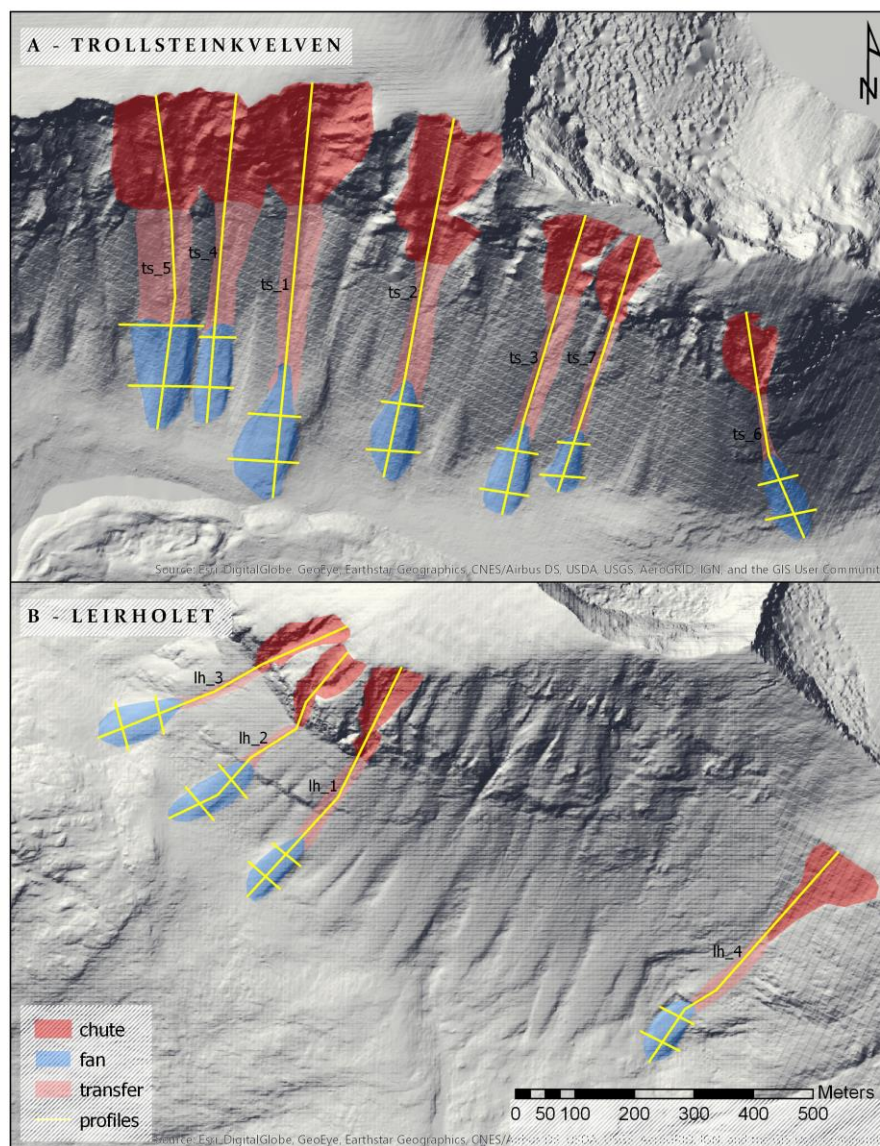


Figure 4 DEM of the study sites in (A) Trollsteinkvelven and (B) Leirholet defining the areas classified as chutes, fans and transfer zones, and the location of long- and cross-profiles.

The following parameters were calculated: the *area* of the chute, transfer zone and fan based on their respective polygons; the *length* of each landform assemblage defined as the longest axis downslope for all three polygons combined; the *maximum width* of the fan, based on visual interpretation of the main breaks of slope along the cross profile, the *maximum slope angle* of the three zones based on the longest axis of each polygon; and the *slope* of the eastern and western flanks of the distal part of the fan.

To establish the volumes of the fan, chute and transfer zones, we tried two different approaches: the first based on an artificially calculated reference surface based on raster interpolation; the second based on geometric approximation to the shapes of the three zones. We found that raster interpolation rendered a better fit to the topography and smaller uncertainties. Although it provided results that best matched field observations, the interpolation method also has its limitations, notably relating to the differentiation of the three zones, the recognition of bedrock, the delineation of individual fans, and their separation from adjacent talus.

In order to calculate the reference surface, the polygons for fan, transfer zone and chute were used to clip the DEM. The clipping tool removed the current surface and the resulting gaps in the raster map were subsequently filled by employing a nearest neighbour algorithm, using a window of 10 x 10 cells. The lowest cell value was selected for the reference surface of the fan and the highest cell value for the chute and transfer zone (cf. Watson and Philip 1987). Fifteen iterations were required to fill the gaps in the Trollsteinkvelven map and ten iterations for the Leirholet area. In order to calculate the volumes, the cut and fill tool of ArcGIS Pro (ESRI 2017) was used to subtract the present-day surface from the newly generated reference surfaces.

Results

Geomorphometrics

The overall length of each long-profile ranges from 394 to 701 m and the three zones are of approximately equal length with the length of the fan zone varying between 108

and 232 m (Figure 5). Slope angles decline consistently down the chute, transfer and fan zones, from 19-23° to 14-21° and 8-15°, respectively, demonstrating the characteristic convexity of each long profile and reflecting the effect of snow-avalanche run-out in the fan zone.

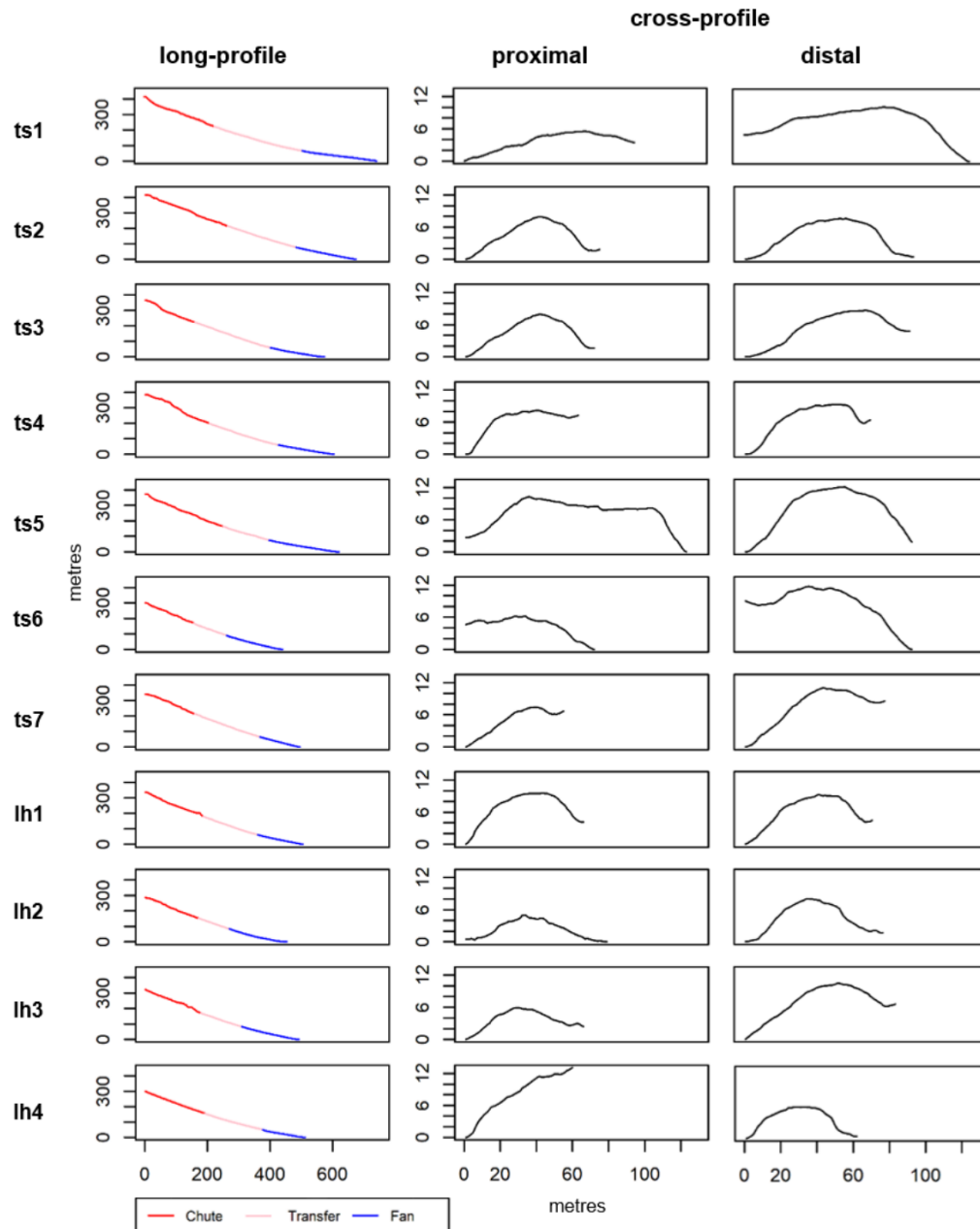


Figure 5 Long- and cross-profiles from Trollsteinkvelven (ts 1-7) and Leirholet (lh 1-4). Note the west side is to the left in the cross-profiles.

The narrow widths (49-96 m), steep sides (4.1-10.7° on the west side and 3.9-10.4° on the east side) and flat tops in some cases (Figure 5) of the fan zones are typical of snow-avalanche fans of the roadbank type. Although the asymmetry in these cross-profiles is not consistent, eight out of 11 west-side slopes are steeper than the corresponding east-side slope, which may reflect prevailing westerly winds and snow-bed accumulation leading to deflection of snow-avalanche tracks as suggested by Rapp (1959). Lack of more consistent asymmetry in these fans appears to be due to the dominance of local topographic variability.

Results of the volume calculations for the three zones are summarized in Table 1. Notable features of these data include, firstly, large variations in the values which, in part, reflect natural variability but are also affected by the limitations of the methodology noted above. Secondly, the very large volume of the chutes relative to that of the transfer zones, demonstrates that the chutes are the major source of the boulders in the fans. Thirdly, the volume of 10 of the fans is 22.1 to 97.5 % less than the combined volume of the chutes and transfer zones, which is equivalent to 15.5 to 68.3 % in terms of rock volume when a voids fraction (porosity) of 30 % for the fans is taken into account (cf. Sass and Wollny 2001; Hungr and Evans 2004; Wilson, 2009; Sandøy et al. 2017). Some of the rock material eroded from the chutes is therefore ‘missing’ from these fans. Fourthly, the large volume of the fan at Trollsteinkvelven 5 is anomalous in exceeding the combined volume of the chute and transfer zone.

Table 1 Summary of volume calculations for 11 chutes, transfer zones and fans.

| Fan No. | Chute (<i>C</i>) (m ³) | Transfer (<i>T</i>) (m ³) | Fan (<i>F</i>) (m ³) | (<i>C</i> + <i>T</i>) (m ³) | 100F/(<i>C</i> + <i>T</i>) (%) | Corrected* (%) |
|-------------------|---|--|---------------------------------------|--|-------------------------------------|-------------------|
| Trollsteinkvelven | | | | | | |
| 1 | 91,078 | 2,884 | 67,186 | 93,962 | 71.5 | 50.1 |
| 2 | 303,092 | 4,762 | 67,081 | 307,854 | 21.8 | 15.3 |
| 3 | 100,193 | 2,312 | 39,943 | 102,505 | 39.0 | 27.3 |
| 4 | 42,111 | 9,721 | 50,526 | 51,832 | 97.5 | 68.3 |
| 5 | 45,283 | 22,226 | 129,775 | 67,509 | 192.2 | 134.6 |
| 6 | 79,713 | 331 | 41,279 | 80,044 | 51.6 | 36.1 |
| 7 | 58,587 | 475 | 23,079 | 59,062 | 39.1 | 27.4 |
| Leirholet | | | | | | |
| 1 | 91,658 | 914 | 22,419 | 92,572 | 24.2 | 16.9 |
| 2 | 91,430 | 120 | 30,722 | 91,550 | 33.6 | 23.5 |
| 3 | 79,438 | 543 | 35,218 | 79,981 | 44.0 | 30.8 |
| 4 | 101,392 | 720 | 22,597 | 102,112 | 22.1 | 15.5 |

*Corrected percentage is the fan volume as a percentage of the combined volume of the chute and transfer zone, assuming a voids fraction (volume of voids/volume of rock) of 30%

As well as the their typical profiles, major dimensions and slope angles, the fan surfaces are characterized by minor morphological features, such as scattered angular boulders, perched boulders and sediment drapes (cappings) deposited from ablating snow, erosional furrows of various types and debris tails in the lee of boulders produced by avalanche scour of adjacent surface sediments (cf. Rapp 1959; Blikra and Nemec 1998; Jomelli and Francou 2000; Jomelli and Bertran 2001; Sekiguchi and Sugiyama 2003; Owen et al. 2006).

SHD control-point data and calibration equations

R-values used as control points (Table 2) show differences between Trollsteinkvelven and Leirholet sufficient to justify separate calibration equations for the two locations (Figure 6). Mean R-values for the ‘old’ control points differ significantly, with higher values in Trollsteinkvelven (42.90 ± 1.12) compared to Leirholet (38.64 ± 1.11) and non-overlap of their 95% confidence intervals. The difference between the mean R-values for the young control points at Trollsteinkvelven and Leirholet is not statistically significant.

Table 2 Control point Schmidt-hammer R-values from Trollsteinkvelven and Leirholet used in local calibration equations: n = No. of impacts for bedrock surfaces; and n = No. of boulders for boulder surfaces (based on two impacts per boulder).

| Site type | Site age (years) | R-values | | | n* |
|--------------------------|---------------------|----------|----------|-----------|-----|
| | | Mean | σ | 95% CI | |
| <i>Trollsteinkvelven</i> | | | | | |
| Avalanche boulders | 20 | 59.83 | 6.45 | 1.29 | 100 |
| Bedrock outcrops | 9,700 | 42.90 | 9.88 | 1.12 | 300 |
| <i>Leirholet</i> | | | | | |
| Avalanche boulders | 20 | 58.66 | 4.15 | 0.78 | 110 |
| Bedrock outcrops | 9,700 | 38.64 | 38.64 | 1.11 | 300 |

Another notable feature of these control-point R-values, particularly those from the ‘old’ control points, is their relatively high variability as measured by the standard deviation (Table 2) and illustrated by the histograms in Figure 6. This high variability is attributed to lithological variation within the pyroxene-granulite gneiss. The negative skew of the distribution in Trollsteinkvelven and the platykurtic distribution in Leirholet, features that are non-typical for control points, likely reflect the presence of a lithological variant (more abundant in Trollsteinkvelven than in Leirholet) that is relatively resistant to chemical weathering and hence results in relatively high R-values. This would also account for higher mean R-values than have been found for control points of similar age from pyroxene-granulite gneiss and related rock types elsewhere in Jotunheimen (cf. Matthews and Owen 2010; Matthews et al. 2014, 2018).

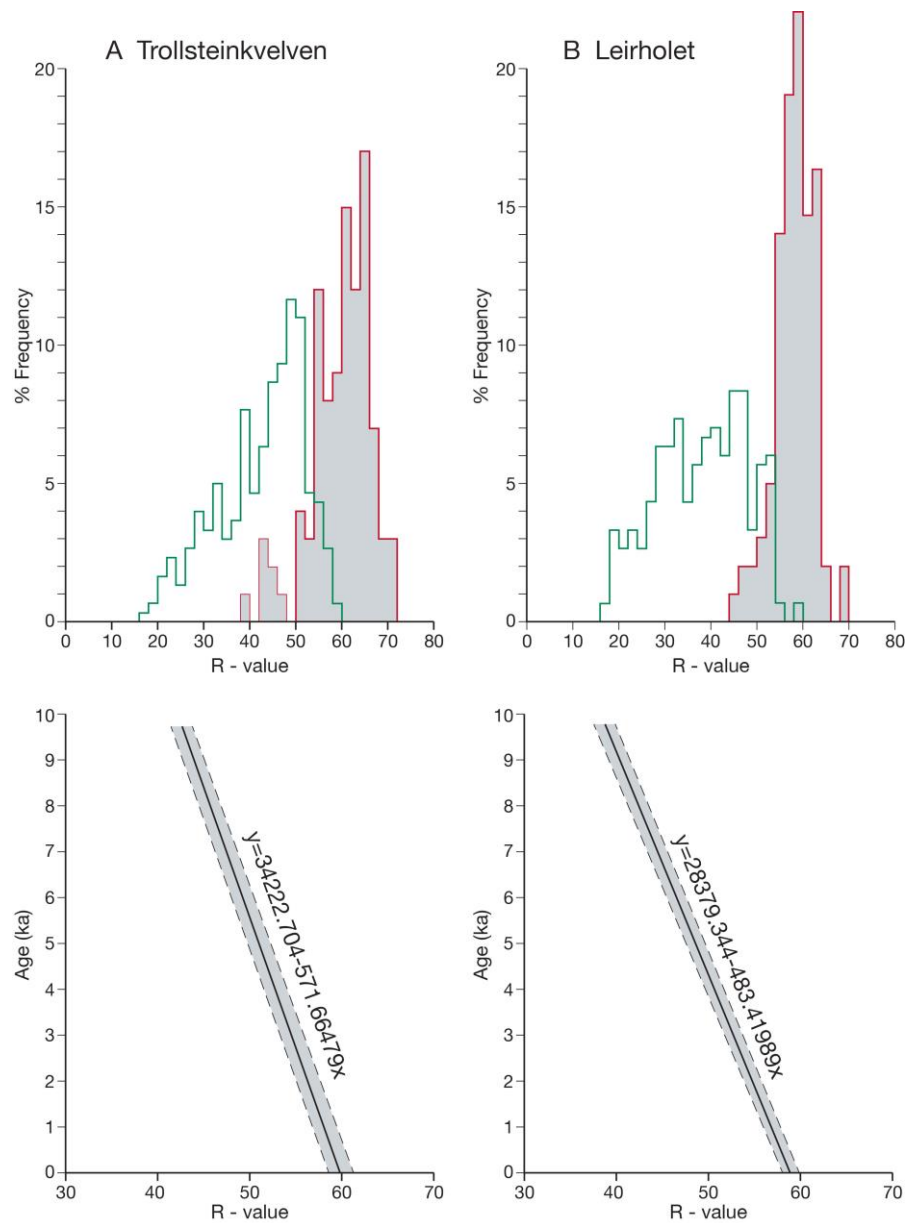


Figure 6 Schmidt-hammer R-value distributions for ‘old’ and ‘young’ control points (upper panels) and the corresponding age calibration equations and calibration curves (lower panels) from (A) Trollsteinkvelven and (B) Leirholet. ‘Young’ control points (surface exposure age 20 years) are shaded; ‘old’ control points (surface exposure age 9.7 ka) are unshaded.

Schmidt hammer R-values and SHD ages

Mean R-values and R-value distributions from the fans (Table 3 and Figure 7) are intermediate in character between those of the ‘old’ and ‘young’ control points, signifying intermediate ages (see below). The seven fans in Trollsteinkvelven are characterized by remarkably similar mean R-values within the range 50.86 ± 1.84 to 52.66 ± 1.58 , all with overlapping 95% confidence intervals. The fans in Leirholet,

with the exception of fan 4, have significantly lower mean R-values ranging from 43.30 ± 1.93 to 45.72 ± 1.89 . It is also notable that R-value variability on the fans is much higher than for the ‘young’ control points and almost as high as for the ‘old’ control points. Relatively high R-value variability amongst the boulders can be attributed to a combination of lithological variation and exposure-age variation.

Table 3 Schmidt-hammer R-values and SHD ages from 11 snow-avalanche boulder fans; n = 100 boulders (200 impacts) for each fan.

| Fan No. | R-values | | | SHD age \pm 95% CI (years) | Cc (years) | C3 (years) |
|--------------------------|----------|----------|--------|------------------------------------|---------------|---------------|
| | Mean | σ | 95% CI | | | |
| <i>Trollsteinkvelven</i> | | | | | | |
| 1 | 51.09 | 8.47 | 1.68 | 5020 ± 1180 | 687 | 962 |
| 2 | 50.86 | 9.27 | 1.84 | 5150 ± 1255 | 686 | 1052 |
| 3 | 52.24 | 8.72 | 1.73 | 4360 ± 1210 | 694 | 989 |
| 4 | 51.75 | 8.95 | 1.77 | 4640 ± 1230 | 691 | 1015 |
| 5 | 51.30 | 7.89 | 1.56 | 4895 ± 1130 | 688 | 894 |
| 6 | 51.45 | 8.08 | 1.60 | 4810 ± 1145 | 688 | 916 |
| 7 | 52.66 | 7.97 | 1.58 | 4210 ± 1140 | 696 | 904 |
| <i>Leirholet</i> | | | | | | |
| 1 | 45.72 | 9.51 | 1.89 | 6280 ± 995 | 480 | 869 |
| 2 | 44.51 | 8.30 | 1.65 | 6865 ± 905 | 490 | 758 |
| 3 | 43.30 | 9.78 | 1.94 | 7445 ± 1020 | 499 | 892 |
| 4 | 53.98 | 6.49 | 1.29 | 2285 ± 725 | 414 | 593 |

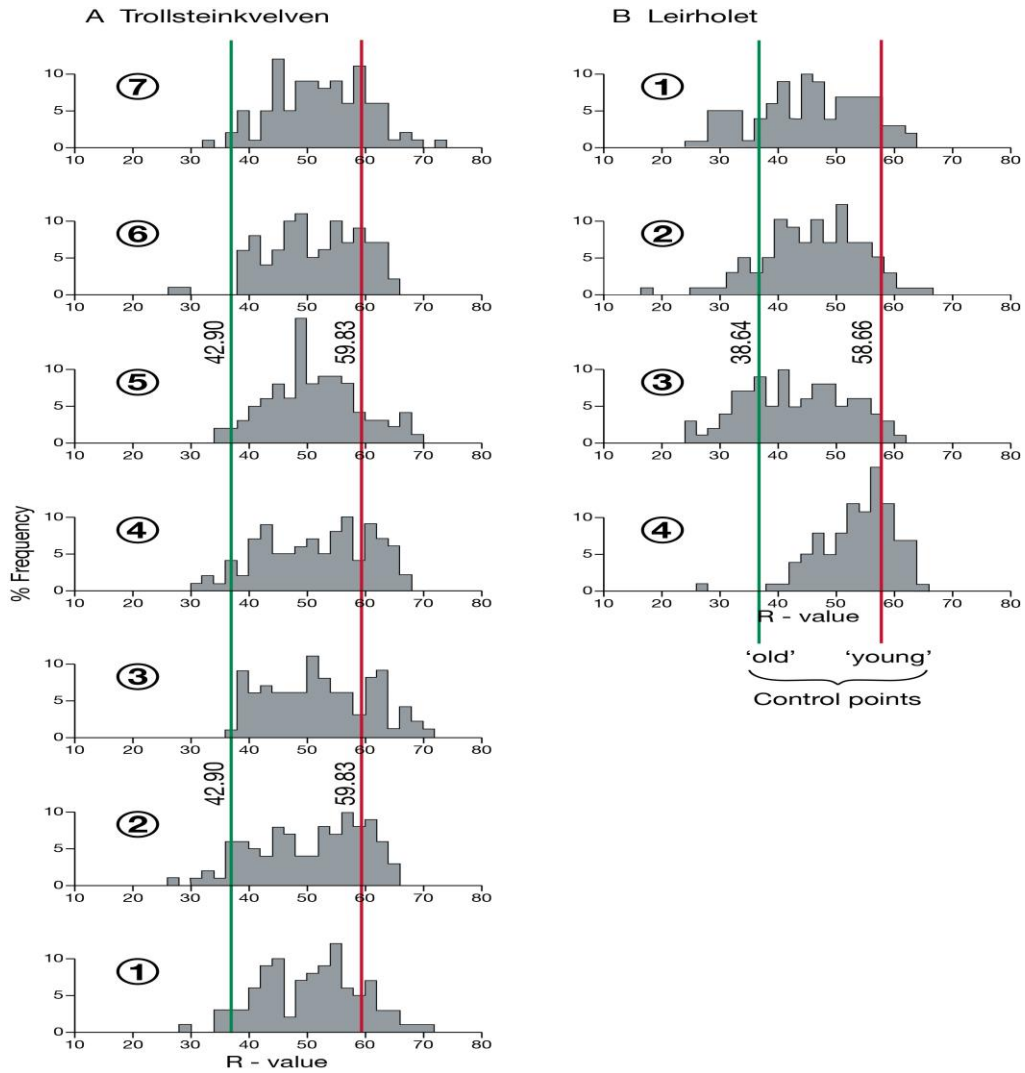


Figure 7 Schmidt-hammer R-value distributions for (A) snow-avalanche fans 1-7 in Trollsteinkvelven, and (B) fans 1-4 in Leirholet. Vertical lines indicate mean R-values for 'old' and 'young' control points.

Calibration of the R-values yielded the SHD ages shown in Table 3 and Figure 8, from which three populations of snow-avalanche boulder fans can be inferred. First, in Trollsteinkvelven, fans 1-7 all fall within the SHD age range 4120 ± 1140 to 5150 ± 1255 years. Second, three of the fans in Leirholet are older, with a SHD age between 6280 ± 995 and 7445 ± 1020 years. The average SHD ages of these two groups are 4715 ± 1185 and 6865 ± 975 years, respectively, a difference of about 2000 years. Third, the SHD age of fan 4 from Leirholet is 2285 ± 725 years, which is at least 4000 years younger than the other fans in Leirholet.

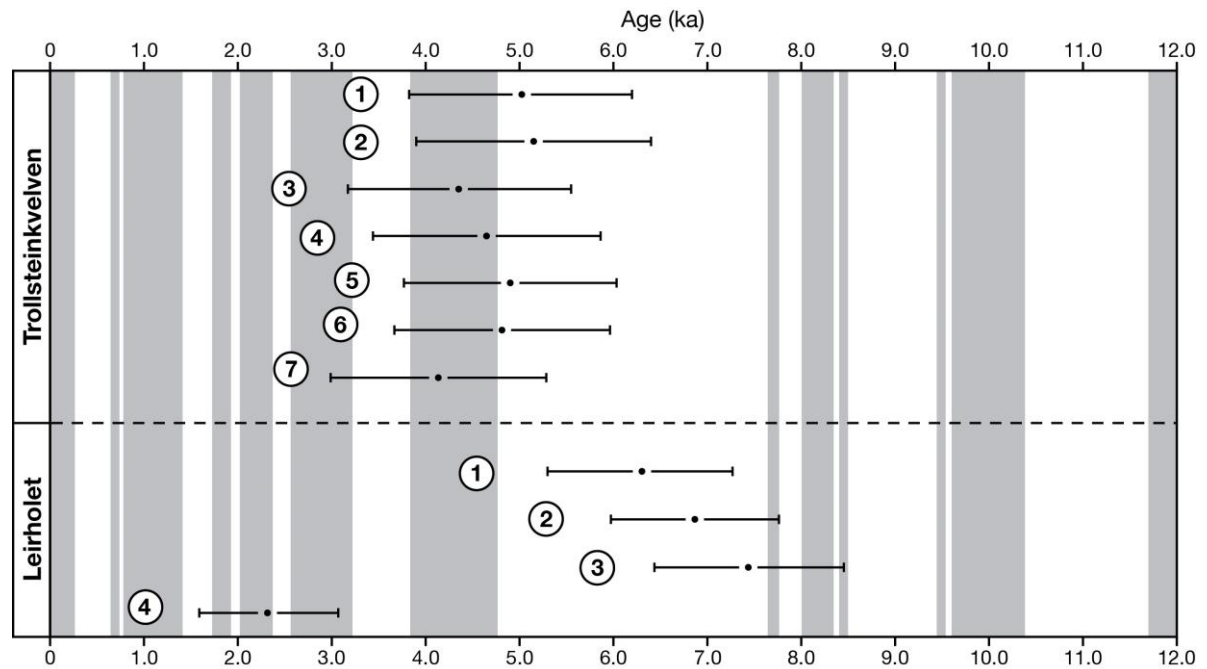


Figure 8 SHD ages (\pm 95% confidence intervals) for seven snow-avalanche fans in Trollsteinkvelven and four fans in Leirholet. Shaded columns represent glacier expansion episodes in the Smørstabbtinden massif (after Matthews and Dresser, 2008) with the addition of the Younger Dryas ending at ~11.7 ka.

Indications of age from lichen-size data

The largest lichens on the fans exceed 400 mm and a large number are >300 mm (Table 4). Environmental conditions on the distal parts of the fans appear favourable for lichen growth and survival, particularly in Trollsteinkvelven, where the mean of the five largest lichens across the seven fans is consistently within the range 320-340 mm. This remarkably low variability between fans seems to justify the southern Norwegian practice of using a mean of the five largest lichens for lichenometric dating: single largest lichens being subject to the inherent unreliability of extremes and use of a larger number leading to underestimates of exposure age from the inclusion of relatively young thalli that colonized the rock surfaces long after the boulders were deposited (Matthews 1994).

Table 4 Maximum diameters of crustose lichens of the *Rhizocarpon* subgenus from 11 snow-avalanche boulder fans.

| Fan No. | Single largest (mm) | 5 largest (mm) | 10 largest (mm) |
|--------------------------|---------------------|----------------|-----------------|
| <i>Trollsteinkvelven</i> | | | |
| 1 | 380 | 330 | 275 |
| 2 | 420 | 330 | 300 |
| 3 | 350 | 320 | 300 |
| 4 | 350 | 330 | 310 |
| 5 | 340 | 320 | 300 |
| 6 | 390 | 330 | 310 |
| 7 | 350 | 340 | 310 |
| <i>Leirholet</i> | | | |
| 1 | 290 | 260 | 250 |
| 2 | 400 | 315 | 280 |
| 3 | 250 | 215 | 200 |
| 4 | 190 | 160 | 150 |

In Leirholet, the largest lichens approach those found in Trollsteinkvelven only at fan 2. The somewhat smaller lichens associated with fans 1, 3 and 4 in Leirholet appear to reflect reduced lichen growth where snowbeds are larger and snow lies longer: optimum conditions for the *Rhizocarpon* subgenus being associated in Jotunheimen with snow cover of intermediate duration (Haines-Young 1983, 1988).

Extrapolation of the available indirect lichenometric dating curves for eastern and central Jotunheimen (Matthews 2005), which were constructed on the basis of the five largest lichens on surfaces deglaciated during recent centuries, suggests that lichens with a diameter of 300 mm indicate surface exposure ages of 1550 and 1510 years in Trollsteinkvelven (eastern Jotunheimen) and Leirholet (central Jotunheimen), respectively. Similarly, the predicted surface exposure ages from lichen diameters of 400 mm is 3320 and 3250 years, respectively. However, these predicted ages cannot be taken at face value as they involve extrapolation far beyond the secure data base of the lichenometric dating curves. Directly measured lichen growth rates (Trenbith and Matthews 2010; Matthews and Trenbith 2011) suggest, moreover, that the age of such large lichens is likely to be no older than ~1000 years. Thus, the lichen-size data should be regarded as relative-age evidence rather than providing independent numerical exposure ages.

Discussion

SHD dating of active landforms and diachronous surfaces

This study adds to an increasingly wide range of results now available from the application of SHD to active and relict landforms of different types in southern Norway (Figure 9) and demonstrates the potential of the technique in the context of active landforms that exhibit diachronous surfaces.

Our SHD ages between 2285 ± 725 and 7445 ± 1020 years, with ten of the 11 fans between 4120 ± 1140 and 7445 ± 1020 years, represent the *average* exposure age of boulders on the distal part of each fan. These surfaces include boulders with both younger and older exposure ages. The exposure ages of the youngest boulders are clearly modern in the sense that they are unweathered with zero exposure age. Relatively young boulders may include those reworked by snow avalanche and/or processes such as debris flow (which are more likely to be active on the proximal parts of the fans). Older generations of boulders are buried beneath the surface boulders. Thus, our SHD ages represent *minimum* estimates of fan surface age.

Interpretation of the SHD ages from the relict landforms in Figure 9 tends to be much simpler as most of them represent synchronous surfaces that became inactive at one point in time or at least over a relatively short interval of time. Most of the landforms that became relict in the early Holocene or earlier accordingly yielded SHD ages that are older than those from our snow-avalanche fans. Those dates that are younger (the flood berms and many of the rock-slope failures) are from the synchronous surfaces of genuinely younger landforms.

The SHD ages from our snow-avalanche fans are older than those from the active snow-avalanche ramparts, ice-cored moraines and pronival ramparts but tend to be younger than those from the cryoplanation terraces (Figure 9). These SHD ages reflect the interval of time that the landforms have been active and the level of activity, especially in recent times. In the case of the snow-avalanche fans, we can deduce that they have been active throughout the Holocene and that current activity levels are low (see below). Recent activity levels are higher for the other landforms and the ice-cored moraines, for example, were particularly active in the Little Ice Age, when glaciers such as Grotbrean in Trollsteinkvelven (see Fig. 3A) were pushing against their proximal moraine slopes (Matthews et al., 2014). The SHD ages of the cryoplanation terraces are distinctly older than the other active landforms mainly because these surfaces develop extremely slowly and only small areas of the terraces are active today (Matthews et al., 2019).

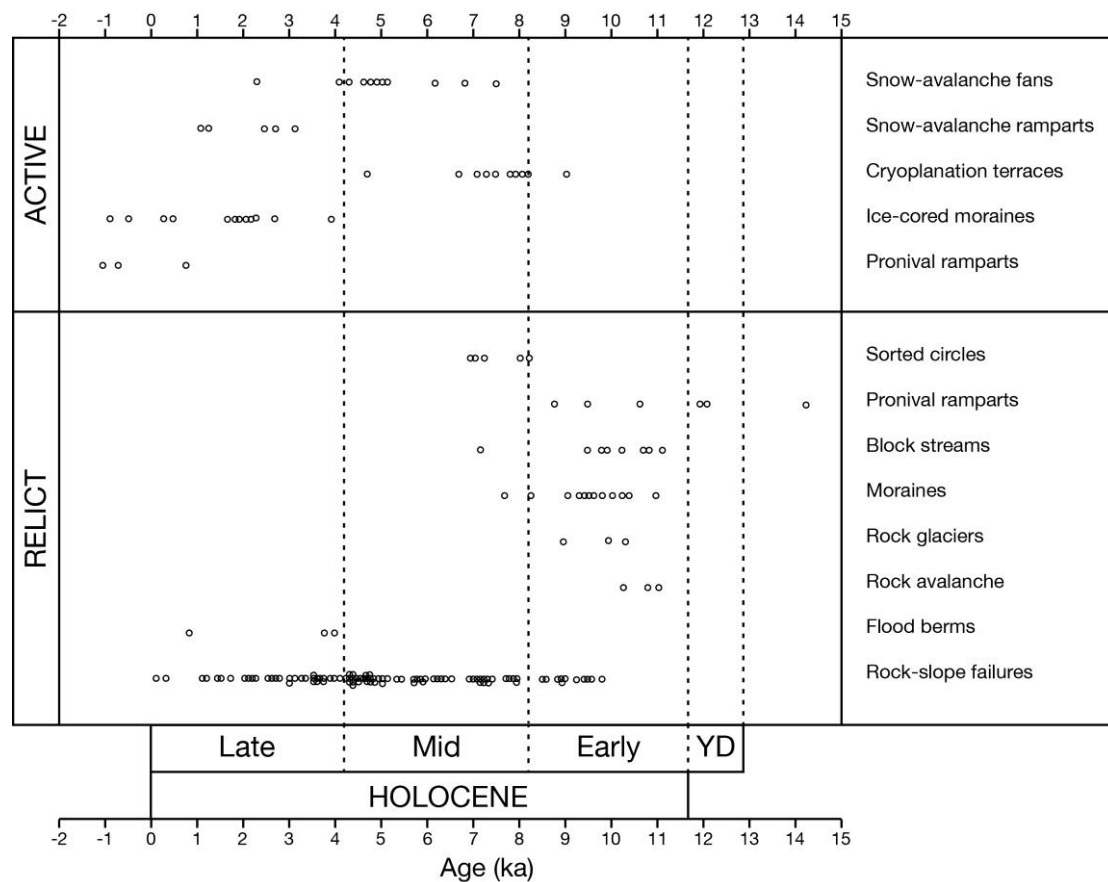


Figure 9 SHD ages from active and relict landforms in southern Norway. Each circle represents a discrete SHD date; confidence intervals of ~500-1000 years are omitted for clarity. Sources: snow-avalanche fans (this paper); snow-avalanche ramparts (Matthews et al. 2015; cryoplanation terraces (Matthews et al. 2019); ice-cored moraines (Matthews et al. 2014); pronival ramparts (Matthews and Wilson 2015; Matthews et al. 2017); sorted circles (Winkler et al. 2016); block streams (Wilson et al. 2016); moraines (Matthews and Winkler 2011); rock glaciers (Matthews et al. 2013, 2017); rock avalanche (Wilson et al. 2019); flood berms (Matthews and McEwen 2013); rock-slope failures (Matthews et al. 2018). Subdivision of the Holocene follow the recommendations of Walker et al. 2012).

Clearly, therefore, with careful interpretation, SHD ages provide useful information in the form of estimates of average ages of the exposed surfaces of landforms, which are also minimum age estimates of the oldest parts of diachronous surfaces. They are less useful, however, as estimates of landform age (defined as the age of the onset of landform formation) because they can be gross underestimates. In the case of our snow-avalanche fans this is due partly to the limited transport load of the avalanches, which leads to the slow rate of burial of surface boulders, and partly to the wide statistical confidence intervals.

Dynamics and development of snow-avalanche boulder fans

As the minimum age estimates for all fan surfaces in Trollsteinkvelven are ~4.1-5.2 ka, and the estimates for three of the four in Leirholet are ~6.3-7.5 ka, and there is a relatively large volume of sediments beneath the surface, these fans must have developed largely during the early- to mid Holocene. The antiquity of the surface material, especially at the three oldest Leirholet fans, suggests, moreover, very little later reworking either by snow avalanches or other processes, a condition that is supported by the scarcity of evidence relating to debris-flow activity on the fan surfaces today. Debris-flow levées and lobes were observed only at Leirholet 3. Yet the SHD age of 2285 ± 725 years for fan 4 in Leirholet indicates a significantly younger age than for the other fans, which demonstrates higher late-Holocene levels of deposition by snow-avalanches in this one case where site conditions seem to have been particularly conducive (see below).

Together with the lichenometric evidence and the observed scarcity of fresh, unweathered boulders on the fan surfaces, the antiquity of the SHD ages point to fan development as a result of small additions of boulders from snow avalanching, rather than a lower frequency of high-magnitude depositional events. Large additions of boulders in recent times would have resulted in much younger SHD ages. The origin of the boulders in the fans is bedrock and regolith from up-slope, mainly from the chutes, where cornice-fall avalanches, slab avalanches, loose-snow avalanches and slush avalanches may occur with variable frequency (cf. Eckerstorfer and Christiansen 2011; Eckerstorfer et al. 2013; Laute and Beylich 2014). Rock-slope failures are likely to have contributed to the large volume of the chutes and hence to a substantial part of the volume of the fans, not all of which can be attributed simply to snow-avalanches. Smaller-scale rockfalls have also clearly to be considered as evinced by the extent of talus development between the fans (see Fig. 1).

That fan volume in all but one case (Trollsteinkvelven 5) is exceeded by the combined volume of the chute and transfer zones, is indicative of an appreciable erosion of chutes that is likely to have taken place in pre-Holocene times. The location

of the fans and their slope-foot and valley-floor sites must have been covered by the Younger Dryas Ice Sheet, which is likely to have eroded any fans that had developed at these sites previously. This would have provided a '*tabula rasa*' for fan development. The thickness of this ice sheet is uncertain (Goehring et al., 2008; Nesje, 2009; Mangerud et al., 2011; Hughes et al. 2016; Stroeven et al. 2016) but it may not have been sufficient to cover the upper slopes at both Trollsteinkvelven and Leirholet, which rise to >2000 m a.s.l. Periglacial weathering and erosion above the elevation of the Younger Dryas Ice Sheet therefore provides a potential explanation for the excess volume of the chutes (i.e. the larger volume of bedrock eroded from the chutes than is present in the fans). It is also possible that some chute erosion also occurred pre-Last Glacial Maximum with subsequent preservation of chutes beneath a thin cold-based ice sheet (cf. Kleman, 1994; Hättestrand and Stroeven, 2002; Juliussen and Humlum, 2007; Marr et al., 2018).

The earliest phase of fan evolution probably began immediately after deglaciation at ~9.7 ka, when glacial unloading and debuitressing, paraglacial stress-release jointing, and enhanced hydrostatic pressure from groundwater in rock joints following thawing of bedrock, would all have had the potential to weaken and destabilize the bedrock cliffs, and hence supply coarse debris for snow-avalanche transport (see, for example, Fischer et al. 2006; Cossart et al. 2008; McColl 2012; Ballantyne et al. 2014; Deline et al. 2015). Recently-deposited till would also have been available on the slopes in the snow-avalanche source areas at that time and would have contributed to the debris load of the snow-avalanches. However, due to the steepness of the slopes any till or other glacial deposits were unlikely to be extensive and debris supply from such a source would undoubtedly have become rapidly exhausted, leaving avalanche chutes stripped of regolith.

Debris supply is likely to have been enhanced, however, during the Holocene Thermal Maximum (HTM) between about 9.0 and 5.0 ka. Pollen-based temperature reconstructions from Northern Europe (Seppä et al. 2009), sea-surface temperatures in the North Atlantic (Jansen et al. 2008; Eldevik et al. 2014), Norwegian glacier and speleothem records (Lilleøren et al. 2012) and pine tree limits in the Scandes

Mountains (Dahl and Nesje 1996) all indicate prolonged relatively high temperatures during the HTM with peak temperatures that may have reached up to 3.5 °C higher than at present in eastern Jotunheimen (Velle et al. 2010). Higher temperatures are likely to have triggered active-layer thawing and permafrost degradation in the south-facing slopes of Trollsteinkvelven and Leirholet with an increase in the frequency of rockfalls and rock-slope failures, as argued for the surrounding valleys by Matthews et al. (2018). However, less is known about temporal patterns of precipitation or their effects on the frequency and magnitude of snow avalanches

Significantly older SHD ages for three of the Leirholet fans suggests that paraglacial effects on sediment supply were even more important than in Trollsteinkvelven, the effects of the HTM were less prolonged and/or sediment exhaustion occurred earlier. Early- to mid-Holocene SHD ages for almost all of the fan surfaces indicate diminution of debris supply in the late Holocene when there appears to have been comparatively little fan development at both locations. However, century- to millennial-scale climatic variations, such as those indicated in Figure 8, seem to have had a relatively minor influence on debris supply, snow-avalanche frequency and fan development during the late Holocene (cf. Blikra and Selvik 1998; Nesje et al. 2007; Vasskog et al. 2011). Finally, renewed permafrost degradation is likely to occur at ever higher elevations in response to global warming trends (Gruber and Haeberli 2007; Lilleøren et al. 2012; Patton et al. 2019), which may lead to acceleration of fan development once again in the future. Indeed, the apparently anomalously young SHD age for Leirholet fan 4 may be an indication that such an impact is already happening.

Conclusions

High-precision SHD was applied to active snow-avalanche boulder fans for the first time and a DEM was used to obtain geomorphometric data relating to the volume of the fans and their associated snow-avalanche chutes and transfer zones. At

Trollsteinkvelven, the seven snow-avalanche fans had consistent SHD ages between 4120 ± 1140 and 5150 ± 1255 years; At Leirholet, the ages from three of the four fans were older (6280 ± 995 to 7445 ± 1020 years). The SHD results, interpreted as the average age of boulders on the diachronous distal surfaces of the fans, demonstrate that deposition on the fans occurred mainly in the early- to mid Holocene, and reflect low late-Holocene deposition rates by snow-avalanches.

DEM analyses revealed that the volume of each fan, with one exception at Trollsteinkvelven, ranged from 22,000 to 67,000 m³ and was less than the volume of each chute (42,000–101,000m³). Again with the one exception, transfer-zone volumes were comparatively small (<10,000 m³) and indicate the low erosivity of the snow avalanches affecting these sites. It is inferred that the excess volume of rock eroded from a combination of the chutes and transfer-zones is accounted for by pre-Holocene erosion of the chutes. This appears to represent subaerial erosion in Younger Dryas times or possibly earlier, when the thickness of the Scandinavian Ice Sheet was insufficient to cover the cliff faces.

Debris supply to the fans in the early Holocene is likely to have been enhanced by paraglacial processes following deglaciation (including glacial unloading and debuttreassing, the development of stress-release jointing, increasing hydrostatic pressure from groundwater in rock joints, and rock-slope failure). Later, in response to climatic warming during the Holocene Thermal Maximum, permafrost degradation probably contributed to the debris load of frequent snow avalanches. The relatively young SHD age obtained from one of the Leirholet fans may represent a similar response to the current global warming trend.

Acknowledgements

Fieldwork was carried out on the Swansea University Jotunheimen Research Expeditions of 2017, 2018 and 2019. We thank Mats and Jonas Hiemstra for

assistance in the field, and Ole Jacob and Tove Grindvold for logistical support. Anna C. Ratcliffe prepared most of the figures for publication, and Atle Nesje and Peter Wilson made useful comments on the manuscript. This paper constitutes Jotunheimen Research Expeditions Contribution No. 214 (see <http://jotunheimenresearch.wixsite.com/home>)

References

Ackroyd P. 1986. Debris transport by avalanche, Torlesse Range, New Zealand. *Zeitschrift für Geomorphologie NF*. 30: 1-14.

André MF. 1996. Rock weathering rates in Arctic and subarctic environments (Abisko Mts, Swedish Lapland). *Zeitschrift für Geomorphologie NF*. 40: 499-517.

Andreassen, LM, Winsvold H. 2012. Inventory of Norwegian Glaciers. Norwegian Oslo: Water Resources and Energy Directorate (NVE).

Ballantyne CK. 2018. Periglacial Geomorphology. Chichester: Wiley.

Ballantyne CK, Harris C. 1994. The Periglaciation of Great Britain. Cambridge: Cambridge University Press.

Ballantyne CK, Wilson P, Gheorghiu D, Rodés À. 2014. Enhanced rock-slope failure following ice-sheet deglaciation: timing and causes. *Earth Surface Processes and Landforms*. 39: 900-913.

Barnett C, Dumayne-Peaty L, Matthews JA. 2000. Holocene climatic change and tree-line response in Leirdalen, central Jotunheimen. *Review of Palaeobotany and Palynology*. 117: 119-137.

Batthey MH. 1965. Layered structures in rocks of the Jotunheimen Complex, Norway. *Mineralogical Magazine*. 34: 35-51.

Batthey MH, McRitchie WD. 1973. A geological traverse across the pyroxene-granulites of Jotunheimen in the Norwegian Caledonides. *Norsk Geologiske Tidsskrift* 53: 237-265.

Bathey MH, McRitchie, WD. 1975. The petrology of the pyroxene-granulite facies rocks of Jotunheimen. *Norsk Geologiske Tidsskrift*. 55: 1-49.

Bell I., Gardner J, de Scally F. 1990. An estimate of snow avalanche debris transport, Kaghan Valley, Himalaya, Pakistan. *Arctic and Alpine Research*. 22: 317-321.

Blikra LH, Nemec W. 1998. Postglacial colluvium in western Norway: depositional processes, facies and palaeoclimatic record. *Sedimentology*. 45: 909-959.

Blikra LH, Selvik SF. 1998. Climatic signals recorded in snow avalanche-dominated colluvium in western Norway: depositional facies successions and pollen records. *The Holocene*. 8: 631-658.

Cossart E, Braucher R, Fort M, Bourlés DL, Carcaillet J. 2008. Slope instability in relation to glacial debuttressing in alpine areas (Upper Durance catchment, southeastern France): evidence from field data and ¹⁰Be cosmic ray exposure ages. *Geomorphology*. 85: 3-26.

Dahl S, Nesje A. 1996. A new approach to calculating Holocene winter precipitation by combining glacier equilibrium-line altitudes and pine-tree limits: a case study from Hardangerjøkulen, central southern Norway. *The Holocene*. 6: 381-398.

Dahl SO, Nesje A, Lie Ø, Fjordheim K, Matthews JA. 2002. Timing, equilibrium-line altitudes and climatic implications of two early-Holocene glacial re-advances during the Erdalen Event at Jostedalsgreen, western Norway. *The Holocene*. 12: 17-25.

de Haas T, Kleinhans MG, Carbonneau PE, Rubensdotter L, Hauber E. 2015. Surface morphology of fans in the high-Arctic periglacial environment of Svalbard: controls and processes. *Earth-Science Reviews*. 146: 163-182.

Decaulne A. 2001. Dynamique des versants et risques naturels dans les fjords d'Islande du nord-ouest, l'impact géomorphologique et humain des avalanches et des debris flows. PhD thesis, University of Clermont II, France.

Decaulne A, Saemundsson T. 2006. Geomorphic evidence for present-day snow-avalanche and debris-flow impact in the Icelandic Westfjords. *Geomorphology*. 80: 80-93.

Deline P, Gruber S, Delaloye R, Fischer L, Geertseema M, Giardino M, Hasler A,

Kirkbride M, Krautblatter M, Magnin F, McColl S, Ravel L, Schoeneich P. 2015. Ice loss and slope stability in high-mountain regions. In: Haeberli W, Whitman C, editors. *Snow and Ice-Related Hazards, Risks and Disasters*. Amsterdam: Elsevier; p. 521-561.

Eckerstorfer M, Christiansen HH. 2011. Topographical and meteorological control on snow avalanching in the Longyearbyen area, central Svalbard 2006-2009. *Geomorphology*. 34: 186-196.

Eckerstorfer M, Christiansen HH, Rubensdotter L, Vogel S. 2013. The geomorphological effect of cornice fall avalanches in the Longyeardalen valley, Svalbard. *The Cryosphere*. 7: 1361-1374.

Eldevik T, Risebrobakken B, Bjune AE, Andersson C, Birks HJB, Dokken TM, Drange H, Glessmer MS, Li C, Nilsen JEØ, Ottera OH, Richter K, Skagseth Ø. 2014. A brief history of climate – the northern seas from the Last Glacial Maximum to global warming. *Quaternary Science Reviews*. 106: 225-246.

ESRI. 2017. ArcGIS Pro 2.1. Redlands, CA: Environmental System Research Institute Inc.

Farbrot H, Hipp TF, Etzelmüller B, Isaksen K, Ødegård RS, Schuler TV, Humlum O. 2011. Air and ground temperature variations observed along elevation and continentality gradients in southern Norway. *Permafrost and Periglacial Processes*. 22: 343-360.

Fischer L, Kååb A, Huggel C, Noetzli J. 2006. Geology, glacier retreat and permafrost degradation as controlling factors of slope stability in a high mountain rock wall. *Natural Hazards and Earth System Sciences*. 6: 761-772.

Freppaz M, Gordone D, Filippa G, Maggioni M, Lunardi S, Williams MW, Zanini E. 2010. Soil erosion caused by snow avalanches: a case study in the Aosta valley (NW Italy). *Arctic, Antarctic and Alpine Research*. 42: 412-421.

Garner J. 1970. Geomorphic significance of avalanches in the Lake Louise area, Alberta, Canada. *Arctic and Alpine Research*. 2: 135-144

Goehring BM, Brook EJ, Linge H, Raisbeck GM, Yiou, F. 2008: Beryllium-10 exposure ages of erratic boulders in southern Norway and implications for the history of the Fennoscandian Ice Sheet. *Quaternary Science Reviews*. 27: 320–336.

Gruber S, Haeberli W. 2007. Permafrost in steep bedrock slopes and its temperature-related destabilization following climate change. *Journal of Geophysical Research*. 112: 1-10.

Haines-Young RH. 1983. Size variation of *Rhizocarpon* on moraine slopes in southern Norway. *Arctic and Alpine Research*. 15: 295-305.

Haines-Young RH. 1988. Size-frequency and size-density relationships in populations from the *Rhizocarpon* subgenus Cern. On moraine slopes in southern Norway. *Journal of Biogeography*. 15: 863-878.

Hättestrand C, Stroeve AP. 2002. A relict landscape in the centre of the Fennoscandian glaciation: geomorphological evidence of minimal Quaternary glacial erosion. *Geomorphology*. 44: 127-143.

Hipp T, Etzel Müller B, Westermann S. 2014. Permafrost in alpine rock faces from Jotunheimen and Hurrungane, southern Norway. *Permafrost and Periglacial Processes*. 25: 1-13.

Hormes A, Blaauw M, Dahl SO, Nesje A, Possnert G. 2009. Radiocarbon wiggle-match dating of proglacial lake sediments – implications for the 8.2 ka event. *Quaternary Geochronology*. 4: 267-277.

Huber TP. 1982. The geomorphology of subalpine snow avalanche runout zones: San Juan Mountains, Colorado. *Earth Surface Processes and Landforms*. 7: 107-116.

Hughes ALC, Gyllencreutz R, Lohne Ø, Mangerud J, Svendsen JL. 2016. The last Eurasian ice sheets – a chronological database and time-slice reconstruction, DATED-1. *Boreas*. 45: 1-45.

Hungr O, Evans SG. 2004. Entrainment of debris in rock avalanches: analysis of a long run-out mechanism. *Geological Society of America Bulletin*. 116: 1240-1252.

Isaksen K, Hauck C, Gudevang E, Ødegård RS, Sollid JL. 2002. Mountain permafrost distribution in Dovrefjell and Jotunheimen, southern Norway, based on BTS and DC resistivity tomography data. *Norsk Geografisk Tidsskrift*. 56: 122-136.

Jansen E, Andersson C, Moros M, Nisancioglu KH, Nyland BF, Telford RJ. 2008. The early to mid-Holocene thermal optimum in the North Atlantic. In: Battarbee RW, Binney HA (editors) *Natural Climate Variability and Global Warming: a Holocene*

Perspective. Chichester: Wiley-Blackwell; p. 128-137

Jomelli V, Bertran P. 2001. Wet snow avalanches in the French Alps: structure and sedimentology. *Geografiska Annaler, Series A (Physical Geography)*. 83A: 15-28.

Jomelli V, Francou B. 2000. Comparing the characteristics of rockfall talus and snow avalanche landforms in an alpine environment using a new methodological approach: Massif des Ecrins, French Alps. *Geomorphology*. 35: 181-192.

Jomelli V, Pech P. 2004. Effects of the Little Ice Age on avalanche boulder tongues in the French Alps (Massif des Ecrins). *Earth Surface Processes and Landforms*. 29: 553-564.

Juliussen H, Humlum O. 2007. Preservation of blockfields beneath Pleistocene ice sheets on Solen and Elgahogna, central eastern Norway. *Zeitschrift für Geomorphologie Supplementband N.F.* 51: 113-138.

Karlén W, Matthews JA. 1992. Reconstructing Holocene glacier variations from glacial lake sediments: studies from Nordvestlandet and Jostedalsbreen-Jotunheimen, southern Norway. *Geografiska Annaler, Series A (Physical Geography)*. 74A: 327-348.

Keylock C. 1997. Snow avalanches. *Progress in Physical Geography*. 21: 481-500.

Kleman J. 1994. Preservation of landforms under ice sheets and ice caps. *Geomorphology*. 9: 19-32.

Korup O, Rixen C. 2014. Soil erosion and organic carbon export by wet snow avalanches. *Cryosphere Discussion*. 8: 1-19.

Laute K, Beylich AA. 2014. Morphometric and meteorological controls on recent snow avalanche distribution and activity on hillslopes in steep mountain valleys in western Norway. *Geomorphology*. 218: 16-34.

Lilleøren KS, Etzelmüller B, Schuler TV, Ginås K, Humlum O. 2012. The relative age of permafrost – estimation of Holocene permafrost limits in Norway. *Global and Planetary Change*. 92-93: 209-223

Luckman BH. 1977. The geomorphic activity of snow avalanches. *Geografiska Annaler, Series A (Physical Geography)*. 59A: 31-48.

Luckman BH. 1992. Debris flows and snow avalanche landforms in the Lairig Ghru, Cairngorm Mountains, Scotland. *Geografiska Annaler, Series A (Physical Geography)*. 74A: 109-121.

Luckman BH. 2013. Talus slopes. In: Elias SA, Mock CJ, editors. *Encyclopedia of Quaternary Science*, 2nd edition, Volume 3. Amsterdam: Elsevier; p. 566-573.

Lutro O, Tveten E. 1996. Geologiske kart over Norge, bergrunnskart Årdal, 1:250,000. Trondheim: Norges Geologiske Undersøkelse.

Magnin F, Etzelmüller B, Westermann S, Isaksen K, Hilger P, Hermanns RL. 2019. Permafrost distribution in steep rock slopes in Norway: measurements, statistical modeling and implications for geomorphological processes. *Earth Surface Dynamics*. 7: 1019-1040.

Mangerud J, Gyllencreutz R, Lohne Ø, Svendsen JI. 2011. Glacial history of Norway. In: Ehlers J, Gibbard PL and Hughes PD, editors. *Quaternary Glaciations – Extent and Chronology: a Closer Look*. Amsterdam: Elsevier; p. 279-298.

Marr P, Winkler S, Löffler J. 2018. Investigations on blockfields and related landforms at Blåhø (southern Norway) using Schmidt hammer exposure-age dating: palaeoclimatic and morphodynamic implications. *Geografiska Annaler, Series A (Physical Geography)* 100A: 285-306.

Matthews JA. 1994. Lichenometric dating: a review with particular reference to ‘Little Ice Age’ moraines in southern Norway. In: Beck C, editor. *Dating in Exposed and Surface Contexts*. Albuquerque: University of New Mexico Press; p. 185-212.

Matthews JA. 2005. ‘Little Ice Age’ glacier variations in Jotunheimen, southern Norway: a study in regionally-controlled lichenometric dating of recessional moraines with implications for climate and lichen growth rates. *The Holocene* 15: 1-19.

Matthews JA, Briffa KR. 2005. The ‘Little Ice Age’: re-evaluation of an evolving concept. *Geografiska Annaler, Series A (Physical Geography)*. 87A: 17-36.

Matthews JA, Dresser PQ. 2008. Holocene glacier variation chronology of the Smørstabbtindan massif, Jotunheimen, southern Norway, and the recognition of century- to millennial-scale European Neoglacial events. *The Holocene*. 18: 181-201.

Matthews JA, McEwen LJ. 2013. High-precision Schmidt-hammer exposure-age dating (SHD) of flood berms, Vetlestølsdalen, alpine southern Norway: first application and some methodological issues. *Geografiska Annaler, Series A (Physical Geography)*. 95A: 185-194.

Matthews JA, Owen G. 2010. Schmidt hammer exposure-age dating: development of linear age calibration curves using Holocene bedrock surfaces from the Jotunheimen-Jostedalbreen regions of southern Norway. *Boreas*. 39: 105-115.

Matthews JA, Owen G. 2011. Holocene chemical weathering, surface lowering and rock weakening rates from glacially-eroded bedrock surfaces in an alpine periglacial environment, Jotunheimen, Norway. *Permafrost and Periglacial Processes*. 22: 279-290.

Matthews JA, Trenbith HE. 2011. Growth rate of a very large crustose lichen (*Rhizocarpon* subgenus) and its implications for lichenometry. *Geografiska Annaler, Series A (Physical Geography)*. 93A: 27-39.

Matthews JA, Vater AE. 2015. Pioneer zone geo-ecological change: observations from a chronosequence on the Storbreen glacier foreland, Jotunheimen, southern Norway. *Catena*. 135: 219-230.

Matthews JA, Wilson P. 2015. Improved Schmidt-hammer exposure ages for active and relict pronival ramparts in southern Norway, and their palaeoenvironmental implications. *Geomorphology*. 246: 7-21.

Matthews JA, Winkler S. 2011. Schmidt-hammer exposure-age dating (SHD): application to early-Holocene moraines and a reappraisal of the reliability of terrestrial cosmogenic-nuclide dating (TCND) at Austanbotnbreen, Jotunheimen, Norway. *Boreas* 40, 256-270.

Matthews JA, Berrisford MS, Dresser PQ, Nesje A, Dahl SO, Bakke J, Birks HJB, Lie Ø, Dumayne-Peaty L, Barnett C. 2005. Holocene glacier history of Bjørnbreen and climatic reconstruction in central Jotunheimen, southern Norway, based on proximal glaciofluvial stream-bank mires. *Quaternary Science Reviews*. 24: 67-90.

Matthews JA, Dahl SO, Dresser PQ, Berrisford M.S, Lie Ø, Nesje A, Owen G. 2009. Radiocarbon chronology of Holocene colluvial (debris-flow) activity at Sletthamn, Jotunheimen, southern Norway: a window on the changing frequency of extreme climatic events and their landscape impact. *The Holocene*. 19: 1107-1129.

Matthews JA, Nesje A, Linge H. 2013. Relict talus-foot rock glaciers at Øyberget, Upper Ottadalen, Southern Norway: Schmidt hammer exposure ages and palaeoenvironmental implications. *Permafrost and Periglacial Processes*. 24: 336-346.

Matthews JA, Winkler S, Wilson P. 2014. Age and origin of ice-cored moraines in Jotunheimen and Breheimen, Southern Norway: Insights from Schmidt-hammer exposure-age dating. *Geografiska Annaler, Series A (Physical Geography)*. 96A: 531-548.

Matthews JA, McEwen L, Owen G. 2015. Schmidt-hammer exposure-age dating (SHD) of snow-avalanche impact ramparts in southern Norway: approaches, results and implications for landform age, dynamics and development. *Earth Surface Processes and Landforms*. 40: 1705-1718.

Matthews JA, Owen G, Winkler S., Vater, Wilson P, Mourne RW, Hill JL. 2016. A rock surface microweathering index from Schmidt hammer R-values and its preliminary application to some common rock types in southern Norway. *Catena*. 143: 35-44.

Matthews JA, Wilson P, Mourne RW. 2017. Landform transitions from pronival ramparts to moraines and rock glaciers: a case study from the Smørbotn cirque, Romsdalsalpane, southern Norway. *Geografiska Annaler, Series A (Physical Geography)*. 99A: 15-37.

Matthews JA, Winkler S, Wilson P, Tomkins M, Dortch J, Mourne R, Hill JL, Owen G, Vater A. 2018. Small rock-slope failures conditions by Holocene permafrost degradation: a new approach and conceptual model based on Schmidt-hammer exposure-age dating in Jotunheimen, southern Norway. *Boreas*. 47: 1144-1169.

Matthews JA, Wilson P, Winkler S, Mourne RW, Hill JL, Owen G, Hiemstra J, Hallang H, Geary AP. 2019. Age and development of active cryoplanation terraces in the alpine permafrost zone at Svartkampan, Jotunheimen, southern Norway. *Quaternary Research*. 92: 641-664.

McColl ST. 2012. Paraglacial rock-slope stability. *Geomorphology*. 153-154: 1-16.

Millar S. 2013. Mass movement processes in the periglacial environment. In: Giardino J.R., Harbour J.M., editors. *Treatise on Geomorphology Vol. 8, Glacial; and Periglacial Geomorphology*. San Diego CA: Academic Press; p. 374-391.

Moore JR, Egloff J, Nagelisen J, Hunziker M, Aerne U, Christen M. 2013. Sediment transport and bedrock erosion by wet snow avalanches in the Guggigraben, Matter Valley, Switzerland. *Arctic, Antarctic and Alpine Research*. 45: 350-362.

Moses C, Robinson D, Barlow J. 2014. Methods for measuring rock surface weathering and erosion: a critical review. *Earth-Science Reviews*. 135: 141-161.

Nesje A. 2009. Late Pleistocene and Holocene alpine glacier fluctuations in Scandinavia. *Quaternary Science Reviews*. 28: 2119-2136.

Nesje A, Dahl SO. 2001. The Greenland 8200 cal yr BP event detected in loss-on-ignition profiles in Norwegian lacustrine sediment sequences. *Journal of Quaternary Science*. 16: 155-166.

Nesje A, Bakke J, Dahl SO, Lie Ø, Bøe AG. 2007. A continuous, high-resolution 8500-yr snow-avalanche record from western Norway. *The Holocene*. 17: 269-277.

Nesje A, Bakke J, Dahl SO, Lie Ø, Matthews JA. 2008. Norwegian glaciers in the past, present and future. *Global and Planetary Change*. 60: 10-27.

Nicholson DT. 2008. Rock control in microweathering of bedrock surfaces in a periglacial environment. *Geomorphology*. 101: 655-665.

Nicholson DT. 2009. Holocene microweathering rates and processes on ice-eroded bedrock, Røldal area, Hardangervidda, southern Norway. In: Knight J, Harrison S, editors. *Periglacial and Paraglacial Processes and Environments*. Geological Society of London, Special Publication. 320: 29-49.

Ødgård RS, Sollid JL, Liestøl O. 1992. Ground temperature measurements in mountain permafrost, Jotunheimen, southern Norway. *Permafrost and Periglacial Processes* 3: 231-234.

Olsen T, Stahl T, Borella J. 2019. Clast transport history influences Schmidt hammer rebound values. *Earth Surface Processes and Landforms*. (submitted manuscript).

Owen G, Matthews JA, Shakesby RA, He X. 2006. Snow-avalanche impact landforms, deposits and effects at Urdvatnet, southern Norway: implications for avalanche style and process. *Geografiska Annaler, Series A (Physical Geography)*. 88A: 295-307.

Owens I. 2004. Snow avalanches and landforms. In: Goudie A.S., editor. *Encyclopedia of Geomorphology*, Vol. 1. London: Routledge; p. 42-44.

Patton AI, Rathburn SL, Capps DM. 2019. Landslide response to climate change in permafrost regions. *Geomorphology*. 340:116-128.

Proceq. 2004. Operating instructions. Betonprüfhammer N/NR-L/LR. Schwerzenbach, Switzerland: Proceq SA.

QGIS Development Team. 2019. QGIS Geographic Information System. Open Source Geospatial Foundation Project. <http://qgis.osgeo.org>

Rapp A. 1959. Avalanche boulder tongues in Lappland. *Geografiska Annaler*. 41: 34-48.

Rapp A. 1960. Recent development of mountain slopes in Karkevagge and surroundings, northern Scandinavia. *Geografiska Annaler*. 42: 73-200.

Rode M, Kellerer-Pirklbauer A. 2011. Schmidt-hammer exposure-age dating (SHD) of rock glaciers in the Schöderkogel-Eisenhut area, Schladminger Tauern Range, Austria. *The Holocene*. 22: 761–771.

Sanders D. 2013. Features related to snow avalanches and snow glides, Nordkette range (Northern Calcareous Alps). *GeoAlp*. 10: 71-92.

Sandøy G, Oppikofer T, Nilsen B. 2017. Why did the 1756 Tjellefonna rockslide occur? A back-analysis of the largest historic rockslide in Norway. *Geomorphology*. 289: 78-95.

Sass O and Wollny K. 2001. Investigations regarding alpine talus slopes using ground-penetrating radar (GPR) in the Bavarian Alps, Germany. *Earth Surface Processes and Landforms*. 26: 1071-1086.

Sekiguchi T, Sugiyama M. 2003. Geomorphological features and distribution of avalanche furrows in heavy snowfall regions of Japan. *Zeitschrift für Geomorphologie NF*. 130: 117-128.

Seppä, H, Bjune AE, Telford RJ, Birks HJB, Birks HH, Veski S. 2009. Last nine-thousand years of temperature variability in Northern Europe. *Climate Past*. 5: 523-535.

- Shakesby RA, Matthews JA, Owen G. 2006. The Schmidt hammer as a relative-age dating tool and its potential for calibrated-age dating in Holocene glaciated environments. *Quaternary Science Reviews*. 25: 2846-2867.
- Shakesby RA, Matthews JA, Karlén W, Los SO. 2011. The Schmidt hammer as a Holocene calibrated-age dating technique: testing the form of the R-value-age relationship and defining the predicted-age errors. *The Holocene*. 21: 615-628.
- Stahl T, Winkler S, Quigley M, Bebbington M, Duffy B, Duke D. 2013. Schmidt hammer exposure-age dating (SHD) of late Quaternary fluvial terraces in New Zealand. *Earth Surface Processes and Landforms* 38: 1838-1850.
- Stroeven AP, Hättestrand C, Kleman J, Heyman J, Fabel D, Fredin O, Goodfellow BW, Harbor JM, Jansen JD, Olsen L, Caffee MW, Fink D, Lundqvist J, Rosqvist GC, Strömberg B, Jansson KN. 2016. Deglaciation of Fennoscandia. *Quaternary Science Reviews*. 147: 91-121.
- Tomkins MD, Dortch JM, Hughes PD. 2016. Schmidt hammer exposure dating (SHED): establishment and implications for the retreat of the last British Ice Sheet. *Quaternary Geochronology*. 33: 46-60.
- Tomkins MD, Dortch JM, Hughes PD, Huck JJ, Stimson AG, Delmas M, Calvet M, Pallàs R. 2018. Schmidt hammer exposure dating (SHED): rapid age assessment of glacial landforms in the Pyrenees. *Quaternary Research*. 90: 26-37.
- Trenbith HE, Matthews JA. 2010. Lichen growth rates on glacier forelands in southern Norway: preliminary results from a 25-year monitoring programme. *Geografiska Annaler, Series A (Physical Geography)*. 92A: 19-39.
- Vasskog K, Nesje A, Støren EN, Waldmann N, Chapron E, Ariztegui D. 2011. A Holocene record of snow-avalanche and flood activity reconstructed from a lacustrine sedimentary sequence at Oldevatnet, western Norway. *The Holocene*. 21: 597-614.
- Velle G, Bjune AE, Larsen J, Birks HJB. 2010. Holocene climate and environmental history of Brurskardstjørni, a lake in the catchment of Øvre Heimdalsvatnet, south-central Norway. *Hydrobiologia*. 642: 13-34.
- Viles H, Goudie A, Grabb S, Lalley J. 2011. The use of the Schmidt hammer and Equotip for rock hardness assessment in geomorphology and heritage science: a comparative analysis. *Earth Surface Processes and Landforms*. 36: 320-333.

Walker MJC, Berkelhammer M, Björk S, Cwynar LC, Fisher DA, Long AJ, Lowe J, Newnham RM, Rasmussen SO, Weiss H. 2012. Formal subdivision of the Holocene Series/Epoch: a discussion paper by a Working Group of INTIMATE (Integration of ice-core, marine and terrestrial records) and the Subcommission on Quaternary Stratigraphy (International Commission on Stratigraphy). *Journal of Quaternary Science*. 27: 649–659.

Watson DF and Philip GM. 1987. Neighborhood based interpolation. *Geobyte* 2: 12-16.

White SE. 1981. Alpine mass movement forms (noncatastrophic): classification, description and significance. *Arctic and Alpine Research*. 13: 127-137.

Wilson P. 2009. Storurdi: a late Holocene rock-slope failure (Sturzstrom) in the Jotunheimen, southern Norway. *Geografiska Annaler, Series A (Physical Geography)*. 91: 47-58.

Wilson P, Matthews JA, Mørne RW. 2016. Relict blockstreams at Insteheia, Valldalen-Tafjord, southern Norway: their nature and Schmidt-hammer exposure age. *Permafrost and Periglacial Processes* 28, 286-297

Wilson P, Linge H, Matthews JA, Mørne RW, Olsen J. 2019. Comparative numerical surface exposure-age dating (^{10}Be and Schmidt hammer) of an early-Holocene rock avalanche at Alstadjellet, Valldalen, southern Norway. *Geografiska Annaler, Series A (Physical Geography)*. 101A: 293-309.

Winkler S. 2014. Investigation of late-Holocene moraines in the western Southern Alps, New Zealand, applying Schmidt-hammer exposure-age dating (SHD). *The Holocene*. 24: 48-66.

Winkler S, Lambiel C. 2018. Age constraints of rock glaciers in the Southern Alps/New Zealand – exploring their palaeoclimatic potential. *The Holocene*. 28: 778-790.

Winkler S, Matthews JA. 2014. Comparison of electronic and mechanical Schmidt-hammers in the context of exposure-age dating: are Q- and R-values interconvertible? *Earth Surface Processes and Landforms*. 39: 1128-1136.

Winkler S, Matthews JA, Mørne RW, Wilson P. 2016. Schmidt-hammer exposure ages from periglacial patterned ground (sorted circles) in Jotunheimen, Norway, and their interpretive problems. *Geografiska Annaler, Series A (Physical Geography)*. 98A: 15-37.

Winkler S, Matthews JA, Haselberger S, Hill JL, Mourne RW, Owen G, Wilson P. 2020. Schmidt-hammer exposure-age dating (SHD) of sorted stripes on Juvflye, Jotunheimen (central South Norway): morphodynamic and palaeoclimatic implications. *Geomorphology*. *In press*.